CrossMark

ORIGINAL PAPER

Phosphorhydrazides as urease and acetylcholinesterase inhibitors: biological evaluation and QSAR study

Lida Asadi[2] · Khodayar Gholivand[1] · Karim Zare[2]

Abstract New phosphorhydrazide compounds (**1–7**, **13**, **15–16**) and thiophosphorhydrazide (**14** and **17**) were synthesized and characterized by ^{31}P, ^{13}C, ^{1}H NMR and IR spectroscopy. Furthermore, the crystal structure of compound $(C_6H_5NH)(C_6H_5O)P(O)(NH–NH_2)$ (**2**) was investigated. The activities of derivatives on acetylcholinesterase (AChE) and urease were determined. Quantitative structure–activity relationship (QSAR) was used to understand the relationship between molecular structural features and inhibitory. DFT–QSAR models for enzymes demonstrated the importance of E_{LUMO} parameter in describing the anti-AChE and anti-urease activities of the synthesized compounds. The correlation matrix of QSAR models and docking analysis confirmed that electrophilicity descriptor can control the influence of the polarizability properties of N–H functional group of PAH derivatives in the inhibition of enzymes.

Keywords Phosphorhydrazide · Crystal structure · Urease inhibitor · Anti-AChE · QSAR

Introduction

Urease catalyzes the hydrolysis of urea in plants, algae, fungi, and several microorganisms [1, 2], in the final step of organic nitrogen mineralization to produce ammonia and carbamate. The carbamate produced during this reaction spontaneously decomposes, at physiological pH, to give a second molecule of ammonia and bicarbonate [3–6]. The hydrolysis of the reaction products causes an abrupt overall pH increase, the major cause for the negative side effects of the action of urease both for human and animal health, and for agriculture. Urease inhibitors have also been proposed to control urea hydrolysis in soil [6–16]. In particular, compound with the P(X)–NH2 segment (X = O, S) have received considerable attention as urease inhibitors. The most effective inhibitors are substituted both thiophosphinicamide and phosphinicamide families. Many phosphoramide compounds are the most effective compounds currently available to retard the hydrolysis of urea fertilizer in soil and to decrease ammonia volatilization and nitrite accumulation in soils treated with urea. (Thio)phosphoramide inhibited urease by forming a chelated complex with the nickel ion in the active site of enzyme. Phosphoramide acts as urease inhibitors by coordinating itself to the nickel ions of active site [15]. The oxygen or sulfur atoms and amide group of the inhibitor molecule are engaged in the formation of a bridge between the Ni(1) and Ni(2) ions. In this work, we have compared the effectiveness of new (thio)phosphorhydrazide compounds (**1–17**) to inhibit jack bean urease toward (thio)phosphoramides. In addition, we carried out quantitative structure–activity relationship (QSAR) studies on the aforementioned derivatives to gain an understanding of the activity shown by such compounds, to propose its union mode to the urease active site, and to try to create the correlation between the electronic and structural parameters in contrast to the inhibition potency.

✉ Khodayar Gholivand
   gholi_kh@modares.ac.ir

1   Department of Chemistry, Tarbiat Modares University, P.O. Box: 14115-175, Tehran, Iran

2   Department of Chemistry, Islamic Azad University, Science and Research Branch, Tehran, Iran

Materials and methods

Instrument

The enzyme AChE (human erythrocyte; Sigma, Cat. No. C0663) and BChE (bovine erythrocyte, Sigma, Cat. No. B4186), Triton X-100, bovine serum albumin, Acetylcholinesterase (AChE, EC 3.1.1.7), alpha-naphthyl acetate, beta-naphthyl acetate, fast blue RR, DMSO, Sodium dodecyl sulfate (SDS) were all from Sigma-Aldrich. Acetylthiocholine iodide (ATCh, 99 %, Fluka), 5, 5′-dithiobis (2-nitrobenzoic acid)) (DTNB, 98 %, Merck), Na_2HPO_4, NaH_2PO_4 (99 %), (thio)hydrazide, triethylamine (99.5 %, Merck), $CDCl_3$ (99 %, Sigma Aldrich), $(C_6H_5O)P(O)Cl_2$ (99 %, Merck), $(CH_3O)_2P(S)$ Cl, $(CH_3CH_2O)_2P(S)Cl$ and $(CH_3CH_2O)_2P(O)Cl$ (97 %, Sigma Aldrich) were used as supplied. ^1H, ^{13}C, and ^{31}P spectra were recorded on a Bruker Advance DRX 500 spectrometer. ^1H and ^{13}C chemical shifts were determined relative to internal TMS, and ^{31}P chemical shifts were determined relative to 85 % H_3PO_4 as the external standard. Infrared (IR) spectra were recorded on a Shimadzu model IR-60 spectrometer using KBr pellets. Melting points of the compounds were obtained with an electrothermal instrument. UV spectrophotometer was operated using a PERKIN-ELMER Lambda 25. The correlation analysis was performed by the Statistical Package for Social Scientists (SPSS), version 16.0 for Windows [17].

Synthesis

The synthesis pathway of compounds **1**–**17** was represented in Scheme 1.

N-Hydrazino diphenyl amidophosphate (1)

A solution of hydrazine hydrate (2 mmol) in THF was added at 0 °C to a solution of $(C_6H_5O)_2P(O)Cl$ (1 mmol) in THF. After 4 h stirring, the solvent was removed in vacuum and the resulting white powder was washed with distilled water. Powder sample; m.p. 92 °C, ^1H NMR (300.13 MHz, d6–DMSO, 25 °C, TMS); $\delta = 7.38$ (t, 4H), 7.25 (d, 4H), 7.19 (t,2H), 6.87 (d,$^2J_{PNH} = 38.4$ Hz,1H, N–H_{amid}), 3.99 (2H, NH_2) ppm. ^{13}C NMR (75.46 MHz, TMS); $\delta = 150.57$ (d, $^2J_{PC} = 6.3$ Hz, Cipso), 129.72 (s, Cmetha), 124.77 (s, Cpara), 120.50 (d,$^3J_{PC} = 4.6$ Hz, C_{ortho}) ppm.^{31}P NMR (121.49 MHz, d6–DMSO, 25 °C, H_3PO_4 external), $\delta = 1.05$(m) ppm. IR (KBr) $\tilde{v} = 3327$–3211 (N–H), 1217 (P=O), 1071 (P–O), 934 (P–N), 905 (N–N) cm^{-1}.

### N-Hydrazino (O-phenyl)(N-phenyl) amidophosphate (2)

This compound was synthesized similar to the preparation method of compound **1** using of $(C_6H_5O)P(O)(NHC_6H_5)$ Cl [18] instead of $(C_6H_5O)_2P(O)Cl$. Powder sample; m.p. 229 °C, ^1H NMR (500.13 MHz, d6–DMSO, 25 °C, TMS); $\delta = 6.46$ (d, 2 H, $^2J_{PNH} = 32.6$ Hz, NH–NH), 6.84 (t, 1 H, OC_6H_5), 7.14 (t, 1 H, HNC_6H_5), 7.20 (m, 2 H, HNC_6H_5), 7.22 (d, 2 H, OC_6H_5), 7.33 (t, 2 H, OC_6H_5), 7.85 (d, 2 H, $^3J_{PNH} = 8.5$ Hz, NH) ppm. ^{13}C NMR (125.75 MHz, d6–DMSO, 25 °C, TMS); $\delta = 117.37$ (d, $^3J_{PC} = 7.4$ Hz, 2 C, ortho-HNC_6H_5), 120.71 (d, $^3J_{PC} = 4.5$ Hz, 2 C, ortho-OC_6H_5), 124.12 (s, 1 C, para-OC_6H_5), 128.03 (s, 1 C, para-HNC_6H_5), 129.39 (s, 2 C, meta-OC_6H_5), 135.94 (s, 2 C, meta-HNC_6H_5), 143.80 (s, 1 C, ipso-HNC_6H_5), 150.90 (d, $^2J_{PC} = 6.6$ Hz, 1 C, ipso-OC_6H_5) ppm. $^{31}P\{^1H\}$ and ^{31}P NMR (202.45 MHz, d6–DMSO, 25 °C, H_3PO_4 external); $\delta = -6.45$ (s) (d, $^2J_{PNH} = 32.9$ Hz) ppm. IR (KBr): $\tilde{v} = 3225$ (N–H), 3066 (N–H), 1605 (s), 1499 (s), 1219 (P=O), 950 (P–O), 751 (P–N).

N,N′-Di hydrazino phosphoramidic acid 4-chloro phenyl ester (3)

A solution of hydrazine hydrate (4 mmol) in THF was added at 0 °C to a solution of $(p\text{-}ClC_6H_5O)P(O)Cl_2$ (1 mmol) in THF. After 4 h stirring, the solvent was removed in vacuum and the resulting white powder was washed with distilled water. Powder sample; m.p. 171 °C, ^1H NMR (300.13 MHz, d6–DMSO, 25 °C, TMS), $\delta = 7.32$ (d, $^3J_{HH} = 8.6$ Hz, 2H, Ar–H), 7.15 (d, $^3J_{HH} = 9.0$ Hz, 2H, Ar–H), 7.07 (d, $^2J_{PNH} = 31.0$ Hz, 2H, NH), 5.66 (br, 4H, $2NH_2$) ppm. ^{13}C NMR (75.47 MHz, d6–DMSO, 25 °C, TMS), $\delta = 151.21$ (d, $^2J_{PC} = 6.2$ Hz, Cipso), 128.84 (s), 127.06 (s), 121.80 (d, $^3J_{PC} = 4.9$ Hz, C_{ortho}(ppm. ^{31}P NMR (121.49 MHz, d6–DMSO, 25 °C, H_3PO_4 external), $\delta_{ppm} = -5.44$(m) ppm. IR (KBr) $\tilde{v} = 3355$–3207 (N–H), 1210 (P=O), 979 (P–N), 924 (N–N) cm^{-1}.

N,N′-Di hydrazino phosphoramidic acid 4-methyl phenyl ester (4)

This compound was synthesized similar to the preparation method of compound **3** using of $(p\text{-}CH_3C_6H_5O)P(O)$ Cl_2 instead of $(p\text{-}ClC_6H_5O)P(O)Cl_2$. Powder sample; m.p. 153 °C, ^1H NMR (300.13 MHz, d6–$CDCl_3$, 25 °C, TMS); $\delta = 6.98$–7.06 (q, 4H, Ar–H), 6.01 (d, $^2J_{PNH} = 31.9$ Hz, 2H, 2NH), 5.84 (br, 4H, $2NH_2$), 2.26 (s, 3H, p-CH_3) ppm. ^{13}C NMR (75.46 MHz, DMSO, 25 °C, TMS); $\delta = 150.40$ (d, $^2J_{PC} = 6.3$ Hz, C_{ipso}), 131.62 (s), 129.44 (s), 119.80 (d, $^3J_{PC} = 4.8$ Hz, C_{ortho}), 20.26 (s) ppm. ^{31}P
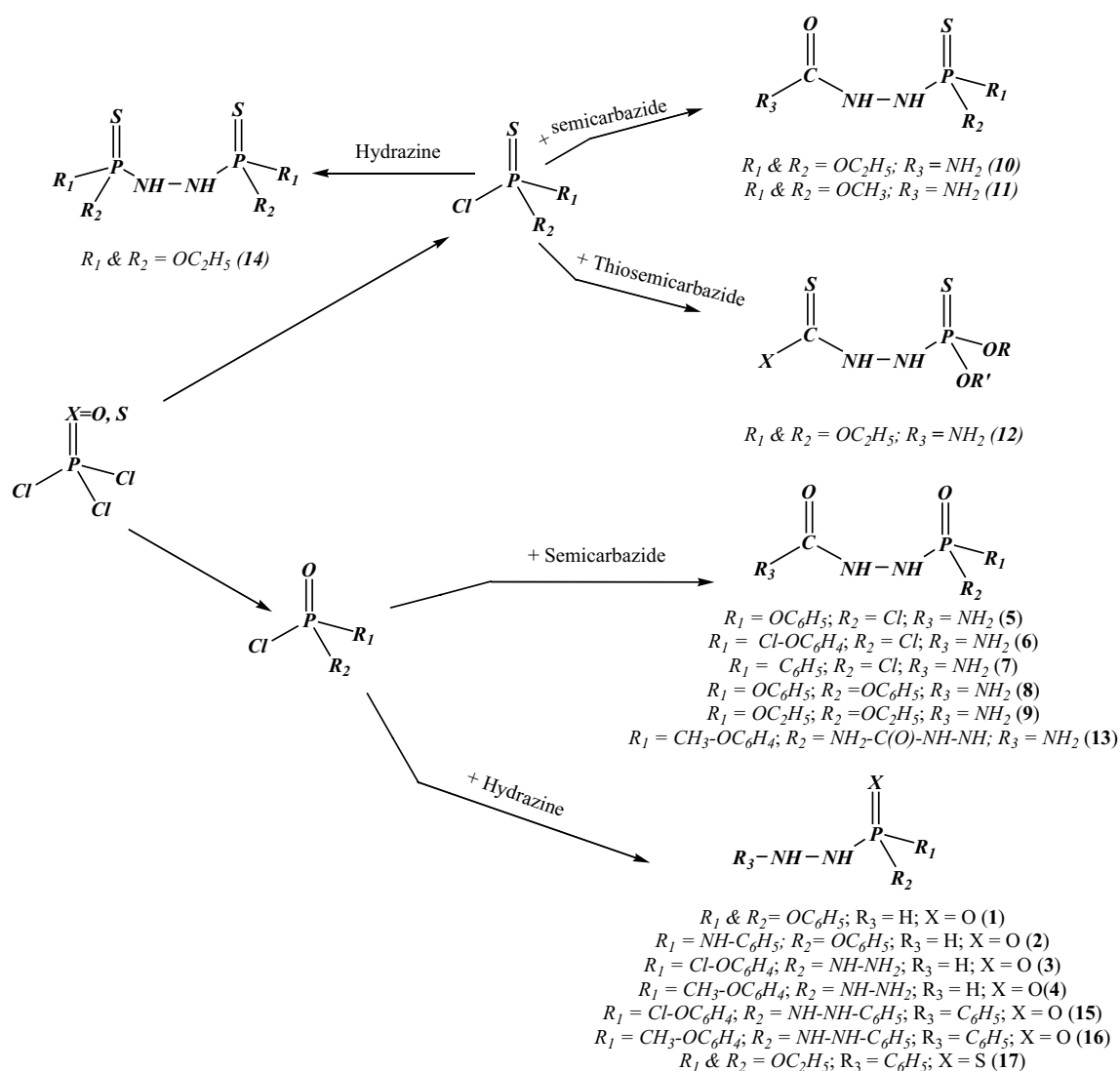
Scheme 1 Preparation of PHA derivatives (**1–17**)

NMR (121.49 MHz, d6–DMSO, 25 °C, H$_3$PO$_4$ external), $\delta = -4.69$(m) ppm. IR (KBr) $\tilde{\upsilon} = 3300$–3250 (N–H), 1214 (P=O), 1034 (P–O), 979 (P–N), 922 (N–N) cm^{-1}.

Chloro N-(semicarbazido) phosphoramidic acid phenyl ester (5)

A solution of semicarbazide (1 mmol) and triethylamine (1 mmol) in THF was added at 0 °C to a solution of (C$_6$H$_5$O) P(O)Cl$_2$ (1 mmol) in THF. After 4 h stirring, the solvent was removed in vacuum and the resulting white powder was washed with distilled water. Powder sample; m.p. 152 °C. ^{1}H NMR (400 MHz, d6–DMSO, 25 °C, TMS); $\delta = 7.63$ (s,1H, N–H$_{amid}$), 7.45 (d, $^2J_{PNH} = 35.6$ Hz,1 H, N–H$_{PNH}$), 7.39–7.15 (5H, m, Ar–H), 5.85 (s,2H, N–H$_{amid}$) ppm. ^{13}C NMR (100.51 MHz, d6–DMSO, 25 °C, TMS); $\delta = 159.60$

(s, C=O), 151.20 (d, C$_{ipso}$, $^2J_{PC} = 6.0$ Hz); 130.00 (s, C$_{para}$), 125.05 (s, C$_{metha}$), 120.82 (d, C$_{ortho}$, $^3J_{PC} = 5.0$ Hz) ppm ^{31}P NMR (161.81 MHz, DMSO,25 °C, H$_3$PO$_4$external), $\delta_{ppm} = 1.98$ (d, $^2J_{PNH} = 34.8$ Hz). IR (KBr) $\tilde{\upsilon} = 3423$–3234 (N–H), 1665 (C=O), 1212 (P=O), 969 (P–N) cm^{-1}.

Chloro N-(semicarbazido) phosphoramidic acid 4-chloro phenyl ester (6)

This compound was synthesized similar to the preparation method of compound **5** using of (p-CH$_3$C$_6$H$_5$O)P(O)Cl$_2$ instead of (C$_6$H$_5$O)P(O)Cl$_2$. Powder sample; m.p. 174 °C, ^{1}H NMR (300.13 MHz, d6–DMSO, 25 °C, TMS); $\delta = 7.64$ (s, 1 H, N–H$_{amid}$), 7.48 (d, $^2J_{PNH} = 35.6$ Hz, 1 H, N–H$_{PNH}$), 7.43–7.24 (4H, m, Ar–H), 5.84 (s, 2 H, NH$_2$) ppm. ^{13}C NMR (75.47 MHz, d6–DMSO, 25 °C, TMS); $\delta = 159.51$

(s, 1 C, C=O), 149.5 7 (d, C_{ipso}, $^2J_{PC}$ = 6.4 Hz).), 129.48 (s, C_{para}), 128.63 (s, C_{metha}), 122.23 (d, $^3J_{PC}$ = 4.7 Hz, C_{ortho}) ppm. ^{31}P NMR (161.83 MHz, d6–DMSO, 25 °C, H_3PO_4 external), δ = 2.08 (d, $^2J_{PNH}$ = 35.6 Hz) ppm. IR (KBr) $\tilde{\upsilon}$ = 3420–3231 (N–H), 1664 (C=O), 1229 (P=O), 965 (P–N) cm^{-1}.

Chloro phenyl N-(semicarbazido) phosphoramidic acid (7)

This compound was synthesized similar to the preparation method of compound **5** using of $(C_6H_5)P(O)Cl_2$ instead of $(C_6H_5O)P(O)Cl_2$. Powder sample; m.p. 199 °C, ^{1}H NMR (300.13 MHz, d6–DMSO, 25 °C, TMS); δ = 7.78–7.40 (5H, m, Ar–H), 7.32 (s, 1 H, N–H$_{amid}$), 7.18 (d, $^2J_{PNH}$ = 27.0 Hz, 1 H, N–H$_{PNH}$), 5.79 (s, 2 H, NH$_2$) ppm. ^{13}C NMR (75.47 MHz, d6–DMSO, 25 °C, TMS); δ = 159.85 (s, C=O), 131.72 (d, C_{ipso}, $^1J_{PC}$ = 16.6 Hz), 131.50 (s, C_{metha}), 129.13 (s, C_{para}), 128.21 (d, C_{ortho}, $^2J_{PC}$ = 13.9 Hz) ppm. ^{31}P NMR (121.49 MHz, d6–DMSO, 25 °C, H_3PO_4 external); δ = 20.93 (d, $^2J_{PNH}$ = 27.0 Hz) ppm. IR (KBr) $\tilde{\upsilon}$ = 3412–3213 (N–H), 1662 (C=O), 1204 (P=O), 973 (P–N) cm^{-1}.

N,N′-Bis(O,O-diethyl phosphorothioyl)hydrazide (14)

A solution of hydrazine hydrate (3 mmol) in THF was added at 0 °C to a solution of $(C_2H_5O)_2P(O)Cl$ (2 mmol) in THF. After 4 h stirring, the solvent was removed in vacuum and the resulting white powder was washed with distilled water. Powder sample; m.p. 84 °C, ^{1}H NMR (300.13 MHz, d6–DMSO, 25 °C, TMS), δ = 7.20 (d, $^2J_{PNH}$ = 38.1 Hz, 2H, N–H), 4.0 (m, 8H, CH$_2$), 1.20–1.25 (t, $^3J_{HH}$ = 7.0 Hz, 12H, CH$_3$) ppm. ^{13}C NMR (75.46 MHz, d6–DMSO, 25 °C, TMS), δ = 62.29 (s, CH$_2$), 15.72 (s, CH$_3$) ppm. ^{31}P NMR (121.49 MHz, d6–DMSO, 25 °C, H_3PO_4 external) ppm. δ = 70.90 (m). IR (KBr) $\tilde{\upsilon}$ = 3390–3251 (N–H), 1024 (P–O), 965 (P–N), 897 (N–N), 795 (P=S) cm^{-1}.

N,N′-bis(phenyl hydrazino) phosphoramidic acid 4-chloro phenyl ester (15)

A solution of phenyl hydrazin (4 mmol) in THF was added at 0 °C to a solution of $(p\text{-ClC}_6H_5O)P(O)Cl_2$ (1 mmol) in THF. After 4 h stirring, the solvent was removed in vacuum and the resulting white powder was washed with distilled water. Powder sample; m.p. 167 °C, ^{1}H NMR (250.13 MHz, d6–D$_2$O, 25 °C, TMS), δ = 7.36 (m, 2 H, N–H$_{PNH}$, $^2J_{PNH}$ = 35.3 Hz), 7.17 (d, 2H, N–H, $^3J_{PNH}$ = 31.8 Hz), 7.13–7.07 (m, 10 H, Ar–H), 6.87–6.84 (m, 4 H, Ar–H), ppm. ^{13}C NMR (75.47 MHz, d6–DMSO, 25 °C, TMS), δ = 150.60 (s, $C_{ipsophenyl}$), 149.99 (s, $C_{ipso\ amine}$), 129.20 (s, C_{metha}), 128.45 (s, $C_{metha\ amine}$), 127.94 (s, C_{para}), 122.47 (d, $C_{para\ amine}$), 118.31 (s, C_{ortho}), 112.56 (d,

$^3J_{PC}$ = 4.0 Hz, $C_{ortho\ amine}$) ppm. ^{31}P NMR (101.25 MHz, d6–DMSO, 25 °C, H_3PO_4 external), δ = 11.46(dt) ppm. IR (KBr) $\tilde{\upsilon}$ = 3318–3267 (N–H), 1211 (P=O), 936 (P–N) cm^{-1}.

N,N′-bis(phenyl hydrazino) phosphoramidic acid 4-methyl phenyl ester (16)

This compound was synthesized similar to the preparation method of compound **15** using of $(p\text{-CH}_3C_6H_5O)P(O)Cl_2$ instead of $(p\text{-ClC}_6H_5O)P(O)Cl_2$. Powder sample; m.p. 196 °C, ^{1}H NMR (250.13 MHz, d6–DMSO, 25 °C, TMS); δ = 7.10 (m, $^2J_{PNH}$ = 34.0 Hz, 2 H, N–H$_{PNH}$), 7.13–7.07 (8 H, Ar–H), 7.09 (d, $^3J_{PNH}$ = 31.3 Hz, 2 H, N–H), 6.89–6.85 (4H, Ar–H), 6.99–6.64 (2H, Ar–H), 2.28 (s, 3 H, p-CH$_3$) ppm. ^{13}C NMR (75.47 MHz, d6–DMSO, 25 °C, TMS); δ = 150.31 (d, $^2J_{PC}$ = 4. 5 Hz, $C_{ipso\ phenyl}$), 149.11 (d, $^3J_{PC}$ = 6.4 Hz, $C_{ipso\ amine}$), 131.26 (s, C_{meta}), 128.43 (s, $C_{metha\ amine}$), 120.46 (s, $C_{para\ amine}$), 118.128 (s, C_{ortho}), 112.558 (d, $^4J_{PC}$ = 4.2 Hz, $C_{ortho\ amine}$), 20.289 (s, p-CH$_3$) ppm. ^{31}P NMR (101.25 MHz, d6–DMSO, 25 °C, H_3PO_4 external); δ = 11.28 (d, $^2J_{PNH}$ = 34.0 Hz). IR (KBr) $\tilde{\upsilon}$ = 3302–3202 (N–H), 1219 (P=O), 937 (P–N) cm^{-1}.

Diethyl N-(phenyl hydrazino) amidothiophosphate (17)

A solution of phenyl hydrazin (2 mmol) in THF was added at at the room temperature to a solution of $(C_2H_5O)P(S)Cl_2$ (1 mmol) in THF. After 4 h refluxing, the solvent was removed in vacuum and the resulting white powder was washed with distilled water. Powder sample; m.p. 73 °C, ^{1}H NMR (300.13 MHz, d6–DMSO, 25 °C, TMS), δ = 7.57 (s, 1 H, N–H), 7.002 (d, $^3J_{HH}$ = 6.0 Hz, 1 H, N–H), 7.004–6.69 (m, 5 H, Ar–H), 4.08–3.98 (m, 10 H, 2C$_2$H$_5$) ppm. ^{13}C NMR (75.46 MHz, d6–DMSO, 25 °C, TMS), δ = 149.73 (m, $C_{ipso\ amine}$), 128.47 (s, C_{para}), 118.25 (d, $^4J_{PC}$ = 5.1 Hz, C_{ortho}), 112.32 (d, $^5J_{PC}$ = 4.2 Hz, C_{meta}), 62.45 (d, $^3J_{PC}$ = 4.9 Hz, CCH$_3$), ppm. ^{31}P NMR (101.25 MHz, d6–DMSO, 25 °C, H_3PO_4 external), δ = 71.94 (m, $^2J_{PNH}$ = 43.2 Hz) ppm. IR (KBr) $\tilde{\upsilon}$ = 3307–2978 (N–H), 802 (P=S), 959 (P–N) cm^{-1}.

Crystal structure determination

X–Ray data of compound **2** were collected on a Bruker SMART 1000 CCD area detector with graphite monochromated Mo-Kα radiation (λ = 0.71073 Å) and refined by full-matrix least-squares methods against F^2 with *SHELXL97* [19]. CCDC 1027079 contain the supplementary crystallographic data for compound **2**. These data can be obtained free of charge via http://www.ccdc.cam.ac.uk/conts/retrieving.html, or from the Cambridge Crystallographic Data Centre, 12 Union Road, Cambridge CB2
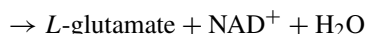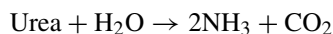
1EZ, UK; fax: (+44) 1223-336-033; or e-mail: deposit@ccdc.cam.ac.uk.

Human ChE assay

Human AChE activity measurements were performed essentially according to the method of Ellman [20]. The reaction was carried out at 37 °C in 70 mM phosphate buffer (Na_2HPO_4/NaH_2PO_4, pH 7.4) containing the AChE enzyme (10 µl volume, diluted 100 times in phosphate buffer, pH 7.4), DTNB (5,5′-dithiobis (2-nitrobenzoic acid)) (10^{-4} M concentration) and ATCh (1.35×10^{-4} M concentration). Each compound was dissolved in dimethyl sulfoxide (DMSO), and then added to buffer for in vitro cholinesterase assays. The highest concentration of DMSO used in the assays was 5 %. In independent experiments without the inhibitor, 5 % DMSO had no effect on the inducing activity of enzyme. The absorbance change at 37 °C was monitored with the spectrophotometer at 412 nm for 3 min and three replicates were run in each experiment. In the absence of inhibitor, the absorbance change was directly proportional to the enzyme level. The reaction mixtures for determination of IC_{50} values, the median inhibitory concentration, consisted DTNB solution, 100 µl; inhibitor, x µl; acetylthiocholin idide (ATCh) solution, 40 µl; phosphate buffer (850-$\times$) µl and hAChE solution, 10 µl.

Urease inhibitory activity

Antiurease inhibition activity was tested by reported protocol [21]. Urea has been determined by the direct method where urea condenses with diacetyl to form a chromagen and an indirect method where ammonia is measured as a product of urease action on urea. The liberated ammonia has been measured using Nessler's reagent and by the Berthelot reaction. Talke and Schubert introduced a totally enzymatic procedure in 1965 utilizing urease and Glutamate Dehydrogenase. The present procedure is based on a modification of their method.

$$Urea + H_2O \rightarrow 2NH_3 + CO_2$$
$$NH_3 + \alpha\text{-Ketoglutarate} + NADH + H^+$$
$$\rightarrow L\text{-glutamate} + NAD^+ + H_2O$$

Urea is hydrolyzed by urease to produce ammonia and carbon dioxide. The liberated ammonia reacts with α-ketoglutarate in the presence of NADH to yield glutamate. An equimolar quantity of NADH undergoes oxidation during the reaction resulting in a decrease in absorbance that is directly proportional to the urea nitrogen concentration in the sample. Concentrations of reagents are NADH 0.3 mM, urease 1500 U/L, glutamate dehydrogenase >1500 U/L, α-ketoglutarate 4.0 mM, buffer pH 8.2 ± 0.1 and phosphoramidate inhibitors. The reconstituted reagent has a reagent blank absorbance less than 1.0 at 340 nm.

Statistical analysis for QSAR model

In order to identify the effect of physicochemical parameters on the AChE inhibition activity, QSAR studies were undertaken using the approach described by Hansch and Fujita. The stepwise multiple linear regression procedure is a common method in QSAR studies for selection descriptors. The MLR method performed by the software package SPSS 16.0 was used for selection of the descriptors. The electronic and structural descriptors are obtained by either the quantum chemical calculations, theoretical and experimental studies. The electronic descriptors include the energy of frontier orbital (E_{HOMO} and E_{LUMO}), electrophilicity (ω), polarizability (PL, the charge difference between the atoms in functional groups) and the net atomic charges (Q). Also hydrophobic coefficient (log$P$), dipole moment (μ) and molecular volume (Mv) are the structural descriptors. E_{HOMO}, E_{LUMO}, ω, P, Q, μ and Mv values are obtained from the DFT results. The logarithm of partition coefficient (log$P$) is measured by the shake–flask and theoretical methods. The toxicities of phosphorhydrazide analogues are expressed in terms of p(IC_{50}) or $-\log(IC_{50})$ as an anti-cholinesterase activity. The descriptor values were related with toxicity using MLR analysis. MLR of descriptors, selected for biological activity, gives rise to the problem of multicollinearity. This problem can be solved using the principal component analysis (PCA). These linear combinations form a new set of variables, namely principal components (PCs), which are mutually orthogonal. The first PC contains the largest variance and the second new variable contains the second largest variance, and so on. The variable selection in this PCA study was performed using the Fisher's weights. The descriptors with higher correlation coefficient and lower correlation ($|r| < 0.5$) to p(IC_{50}) were selected to carry out stepwise MLR analysis and to optimize the QSAR equation [22]. The stable geometry structures of compounds were further fully optimized using the Density functional theory (DFT) at the B3LYP/6–311+G** level of theory. Natural population analysis (NPA) was performed at the same level using the Reed and Weinhold scheme [23]. All quantum chemical calculations were carried out using the Gaussian 03 program package [24].

Results and discussion

Spectral study

Spectroscopy data and phosphorus–hydrogen ($^2J_{PNH}$) coupling constants and $\delta(^{31}P)$ of compounds **1–17** are

Table 1 Selected spectroscopic NMR and IR experimental data of the products

No.	$\delta(^{31}P)_{P=X(O,S)}$	$\delta(^{1}H)_{N–H}$	$^{2}J_{PNH(hydrazide)}$	$\nu_{P=X(O,S)}$	$\nu_{N–H}$	References
1	−5.44	7.07	38.4	1209	3354/3207	a
2	−6.45	7.85	32.9	1218	3224	a
3	−4.69	6.01	31.0	1214	3300/3250	a
4	1.05	6.87	31.9	1217	3327/3210	a
5	1.98	7.45	35.6	1212	3423/3234	a
6	2.08	7.48	35.6	1228	3419/3231	a
7	2.10	7.41	27.0	1203	3412/3212	a
8	2.61	7.82	38.0	1215	3300	[27]
9	6.21	7.02	32.2	1216	3423	[27]
10	69.89	7.39	39.9	790	3445	[27]
11	74.03	7.48	41.2	814	3440	[27]
12	68.66	7.89	35.1	792	3168/3415	[27]
13	8.48	7.27	31.0	1226	3432	a
14	70.90	7.20	38.1	795	3390/3251	a
15	11.46	7.17	35.3	1210	3318	a
16	11.28	7.09	34.0	1218	3302	a
17	71.94	7.57	43.2	802	3307	a

[a] This work

summarized in Table 1. Phosphorus chemical shifts $\delta(^{31}P)$ were observed in the range of −6.45 ppm (**2**) to 74.03 ppm (**11**). As ^{31}P NMR spectra reveal the effect of X on $\delta(^{31}P)$, in P=X moiety this comparison can be made that **10**, **11**, **12**, **14**, **17** compounds consisting P=S moeity show a high upfield shift rather than the compounds with P=O moiety. That is to say, the presence of a sulfur atom leads to the deshielding of phosphorus atom in these derivatives. ^{31}P NMR spectra designate different patterns, compounds **1**, **3**, **4**, **14** indicate singlet pattern, although the rest are appeared as doublets. This splitting pattern arises from the spin couplings between the phosphorus nucleus and NH protons, while a doublet of triplet appeared in compound **15** is achieved from the spin couplings between the phosphorus nucleus and NH and one equivalent hydrogen atoms in amine (NH) group. The $^{2}J_{PNH\alpha}$ was observed for all compounds. The comparison of the $^{2}J_{PNH\alpha}$ values indicate that the compounds with the P=S group (**10**, **11**, **12**, **14**, **17**) have a larger coupling than molecules with P=O group. The greatest and lowest $^{2}J_{PNH\alpha}$ values are observed for **17** ($^{2}J_{PNH\alpha}$ = 43.24 Hz) with the (S)P–NH$_\alpha$–$_\beta$HN–P(S) skeleton and **1** ($^{2}J_{PNH\alpha}$ = 30.99 Hz) with the (O)P–NH$_\alpha$–$_\beta$HN skeleton. The analysis of the IR spectra indicates that the vibrational bands of compounds **1–17** appear in the range of 3300–3445 cm^{-1} for NH group also the fundamental υ(P=X) stretching modes observed in the range of 790 cm^{-1} (P=S) to 1209 cm^{-1} (P=O).

Crystal structures

Colorless single crystal of compound **2** which is suitable for X-ray diffraction analysis was grown from a THF/Chloroform mixture after slow evaporation at room temperature. The crystal data of X-ray analysis is given in Table 2. Molecular structure is shown in Figs. 1 for compound **2**. Compound **2** crystallize in the triclinic crystal system with space group P$_{-1}$. The phosphorus atom has a slightly distorted tetrahedral configuration in compound **2**, that is, the surrounding angles around the P atom are in the range of 95.75(9)°–116.22(9)°. The P=O bond distance is in **2** 1.4812(15) Å. The P–N$_\alpha$ bond distance in **2** 1.6423(18) Å is shorter than the single bond P–N distance of 1.77 Å. The N(3)–H(3NA)…O(1A), N(3)–H(3NA)…N(1), N(1)–H(1N)…N(3A), N(2)–H(2N)…O(1), N(1A)–H(1NA)…N(3), N(2A)–H(2NA)…O(1A) and N(3A)–H(3NC)…O(1) hydrogen bonds produce along a linear direction (Table 3; Fig. 2). The polymeric chains are formed by hydrogen bonds in the crystal lattice with cyclic $R_2^2(8)$ motifs [25] via N(2A)–H(2NA)…O(1A) [d = 2.864(2) Å] (Fig. 2). Three molecules linked in the crystal lattice with cyclic $R_2^3(9)$ motifs which the molecules are connected to each other via two N(2A)–H(2NA)…O(1A) [d = 2.864(2) Å], N(3)–H(3NA)…O(1A) [d = 2.995(3) Å] and N(3)–H(3NA)…O(2) (d = 3.438 Å) hydrogen bonds (Fig. 2). The asymmetric unit is composed of two independent molecules (Fig. 3).

Table 2 Crystallographic data of compound **2**

	2
Empirical formula	C12H14N3O2P
Formula weight	263.23
Temperature (K)	100(2)
Wavelength (Å)	0.71073
Crystal system, space group	Triclinic, *P*-1
Unit cell dimensions	
a (Å)	9.6500(8)
b (Å)	10.2212(9)
c (Å)	13.6586(12)
α (°)	97.589(2)
β (°)	105.344(3)
γ (°)	90.617(2)
V (Å^3)	1286.33(19)
Z, calculated density (Mg m^{-3})	4, 1.359
Absorption coefficient (mm^{-1})	0.212
F(000)	552
Crystal size (mm)	0.35 × 0.35 × 0.05
θ range for data collection (°)	2.01–29.00
Limiting indices	$-13 \le h \le 13$, $-13 \le k \le 13$, $-18 \le l \le 18$
Reflections collected/unique	15,665/6783 [*R*(int) = 0.0281]
Completeness to theta	99.3 %
Absorption correction	Semi-empirical from equivalents
Refinement method	Full-matrix least-squares on *F*^{2}
Data/restraints/parameters	6783/0/326
Goodness-of-fit on *F*^{2}	1.008
Final *R* indices	$R_1 = 0.0520$, $wR_2 = 0.1508$
R indices (all data)	$R_1 = 0.0612$, $wR_2 = 0.1583$
Largest diff. peak and hole (e Å^{-3})	0.547 and −0.440

Biological activity

Anti-AChE activity

To test the experimental anti-acetylcholinesteras (anti-ChE) [22] activity of the synthesized titled compounds, we evaluated the inhibitory potential of titled compounds against AChE enzyme by Ellman assay [20]. The inhibitory ability of selected compounds against AChE were in 2.34 (**11**) to 35.52 (**12**) mM (Table 4). The inhibitory of compound **4** is higher than compound **3** with the (R–C$_6$H$_4$O)(O)P–(NH–NH$_2$)$_2$ (R=CH$_3$, Cl). Comparison of **9** with the (C$_2$H$_5$O)$_2$(O)P–NH–HN–C(O)NH$_2$ structure and **10** with the (C$_2$H$_5$O)$_2$(S)P–NH–HN–C(O)NH$_2$ structure revealed the inhibitory of P=O (**9**) > P=S (**10**) including NH–HN–C(O)NH$_2$ moiety.

Anti-urease activity

Thirteen PAH **1** and **3–14** were evaluated for their inhibitory activities against jack bean urease. Percent inhibition at a 1 mM concentration of compounds **1** and **3–14** was initially determined, and the results were reported in Table 4. Most of the phosphorhydrazides showed good inhibitory activities, especially PAH **9** (IC$_{50}$ = 1.208 mM) and **11** (IC$_{50}$ = 1.611 mM) exhibited potent in vitro inhibitory activities. In general, compounds **5–11** with one NH–HN–C(O)NH$_2$ group exhibited better inhibitory activities than compound **12**. According to Table 4 data, compound **3** exhibited better inhibitory activity than **4**. Compounds **1**, **3**, and **4**, the order of inhibitory activities showed the potency of **3** > **1** > **4**. It was possibly due to the difference between the electro affinities of chlorine, methylen, and proton. Compound **3** with halogen atom in the benzene ring showed better inhibitory activity than those with methyl substitutes.
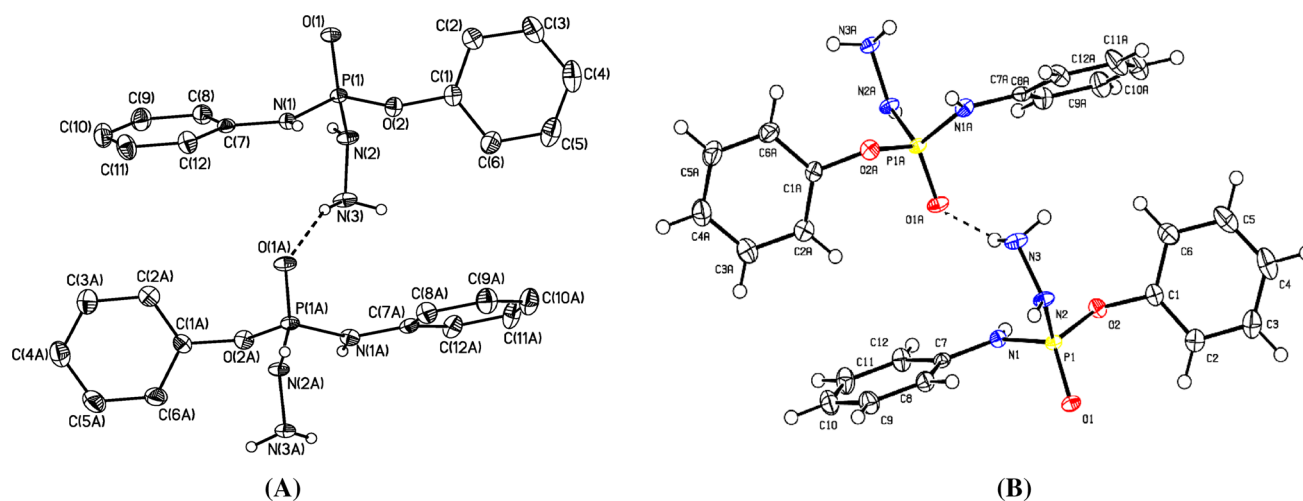

(A)

(B)

Fig. 1 ORTEP representation of compound **2**

Table 3 Hydrogen-bond distances (Å) and angles (°) for **2**

D–H…A	d(D-H)	d(H⋯A)	< DHA	d(D⋯A)
N(3)–H(3NA)…O(1A)[1]	0.93	2.11	158	2.995(3)
N(3)–H(3NA)…N(1)[1]	0.93	2.61	115	3.115(3)
N(1)–H(1N)…N(3A)[2]	0.92	2.05	166	2.956(3)
N(2)–H(2N)…O(1)[3]	0.92	1.99	169	2.903(2)
N(1A)–H(1NA)…N(3)[4]	0.80	2.15	172	2.943(3)
N(2A)–H(2NA)…O(1A)[2]	0.91	2.03	153	2.864(2)
N(3A)–H(3NC)…O(1)[5]	0.85	2.24	168	3.074(3)

Symmetry transformations used to generate equivalent atoms: [1] x, y, z; [2] $-x + 1$, $-y + 1$, $-z + 1$; [3] $-x + 2$, $-y$, $-z + 1$; [4] $-x + 2$, $-y + 1$, $-z + 1$; [5] $x, y + 1, z$
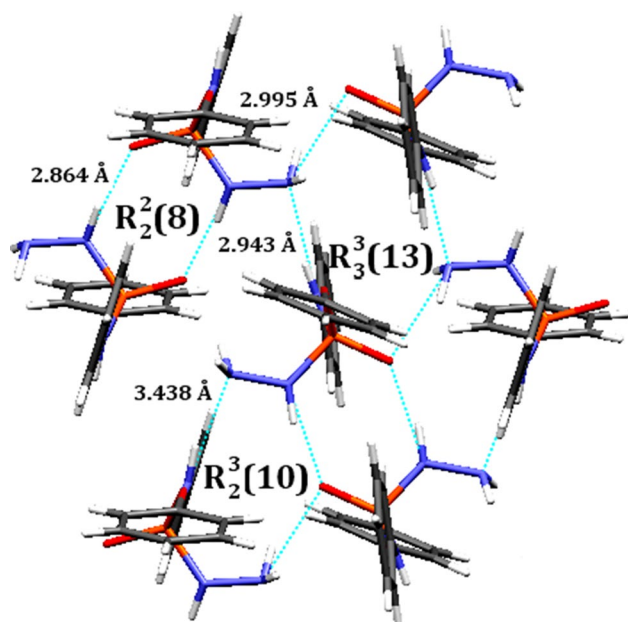
Fig. 2 Graph sets and a model to describe the hydrogen-bonded cluster in compound **2**

QSAR analysis

AChE-QSAR

The docking data provides important basic information including the interaction model, the effective functional groups as well as the electronic and structural properties on the inhibition mechanism. These data can be guide to create and to develop of the QSAR models. So far, no model in literatures has been suggested to explain of the inhibition mechanism PHAs against urease and AChE enzymes. Here, we explain the inhibition mechanism of human AChE and urease by theoretical QSAR models. The electronic and structural descriptors were obtained by quantum chemical calculations (Table 5). The number of the independent variables is more than the tested compounds shown in Table 5.
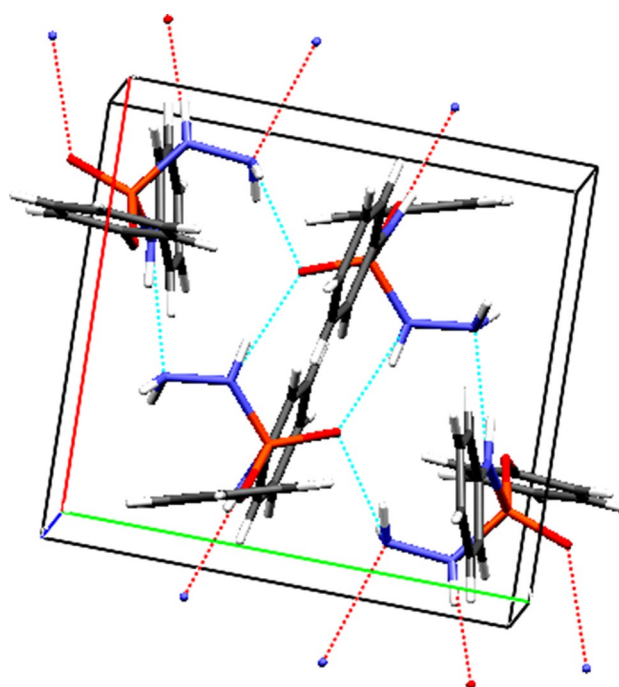

Fig. 3 The asymmetric unit is composed of two independent molecules

Therefore, PCA method was used to reduce the independent variables. The principal components (PCs) as a new set of variables (mutually orthogonal) were obtained by this method. The first PC contains the largest variance and the second PC contains the second largest variance [26]. The variable selection in PCA was performed using the Fisher's weights approach and the results are summarized as the following Eqs. (1a, 1b):

$$PC_1 = -0.340Q_{N(\alpha)} - 0.307Q_{N(\beta)} + 0.308P_{N-H(\alpha)}$$
$$+ 0.378P_{N-H(\beta)} + 0.230E_{HOMO} + 0.431E_{LUMO}$$
$$- 0.419\omega + 0.306\mu + 0.091\log P \qquad (1a)$$

$$PC_1 = -0.319Q_{N(\alpha)} - 0.028Q_{N(\beta)} + 0.254P_{N-H(\alpha)}$$
$$+ 0.157P_{N-H(\beta)} - 0.332E_{HOMO} - 0.133E_{LUMO}$$
$$+ 0.193\omega - 0.270\mu - 0.475\log P \qquad (1b)$$

The results showed the total variance of the first, second and third factor PC as 39.2 and 24.8 %, respectively. Also, from the above equations, it was deduced that the electronic parameters (Q, P, E_{MO} and ω) are predominated from those related to structural parameters ($\log P$ and μ). Consequently, these eleven descriptors with higher correlation coefficient were selected to carry out the stepwise multiple linear regression (MLR) analysis, which led to an optimal QSAR equation based on the anti-AChE potency (Eq. 2):

Table 4 experimental anti-AChE and urease activitis of the PAH analogous for the below moiety
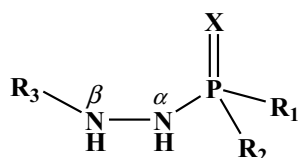
No.	PAH analogous				Biological activity IC_{50} (mM)		References
	R_1	R_2	R_3	X	AChE	Urease	
1	(C_6H_5O)	(C_6H_5O)	H	O	7.006	3.087	a
2	(C_6H_5O)	$(C_6H_5–NH)$	H	O	–	–	a
3	$(Cl–C_6H_4O)$	$NH–NH_2$	H	O	8.690	2.213	a
4	$(CH_3–C_6H_4O)$	$NH–NH_2$	H	O	5.157	50.037	a
5	(C_6H_5O)	Cl	$C(O)NH_2$	O	9.886	7.251	a
6	$(Cl–C_6H_4O)$	Cl	$C(O)NH_2$	O	2.831	4.745	a
7	(C_6H_5)	Cl	$C(O)NH_2$	O	5.370	2.364	a
8	(C_6H_5O)	(C_6H_5O)	$C(O)NH_2$	O	4.020	4.137	[27]
9	(C_2H_5O)	(C_2H_5O)	$C(O)NH_2$	O	7.130	1.208	[27]
10	(C_2H_5O)	(C_2H_5O)	$C(O)NH_2$	S	7.140	2.210	[27]
11	(CH_3O)	(CH_3O)	$C(O)NH_2$	S	2.340	1.611	[27]
12	(C_2H_5O)	(C_2H_5O)	$C(S)NH_2$	S	35.52	94.843	[27]
13	$(CH_3–C_6H_4O)$	$NH–NH–C(O)NH_2$	$C(O)NH_2$	O	–	2.544	a
14	(C_2H_5O)	(C_2H_5O)	$P(S)(C_2H_5O)_2$	S	–	2.623	a
15	$(Cl–C_6H_4O)$	$NH–NH–C_6H_5$	$NH–NH–C_6H_5$	O	–	–	a
16	$(CH_3–C_6H_4O)$	$NH–NH–C_6H_5$	$NH–NH–C_6H_5$	O	–	–	a
17	(C_2H_5O)	(C_2H_5O)	$NH–NH–C_6H_5$	S	–	–	a

a This work

Table 5 Quantum-chemical and theoretical descriptors for compounds computed at B3LYP/6–311+G** level

No.	Electronic									Hydroph.		Steric
	Q_P	$Q_{N(\alpha)}$	$Q_{N(\beta)}$	$P_{P=X}$	$P_{N–H(\alpha)}$	$P_{N–H(\beta)}$	E_{HOMO}	E_{LUMO}	ω	μ	$\log P$	Mv
1	2.359	−0.829	−0.672	−3.455	1.228	1.239	−0.244	−0.019	0.077	6.886	0.04	126.643
3	2.456	−0.887	−0.745	−3.570	1.314	1.152	−0.235	−0.007	0.064	7.521	−0.16	182.634
4	2.452	−0.837	−0.656	−3.535	1.246	1.020	−0.247	−0.014	0.073	8.989	1.71	189.315
5	2.165	−0.812	−0.495	−3.215	1.268	0.903	−0.268	−0.039	0.103	8.146	0.19	150.991
6	2.162	−0.812	0.408	−3.210	1.238	0.904	−0.263	−0.044	0.108	6.926	1.03	179.817
7	1.985	−0.823	−0.496	−3.050	1.246	0.899	−0.280	−0.059	0.131	3.093	−0.26	171.836
8	2.440	−0.800	−0.485	−3.483	1.214	0.864	−0.246	−0.028	0.086	7.067	1.37	245.822
9	2.447	−0.808	−0.485	−3.512	1.221	0.864	−0.270	−0.022	0.086	7.169	0.89	163.656
10	1.963	−0.797	−0.486	−2.562	1.208	0.868	−0.231	−0.022	0.076	7.246	1.25	161.607
11	1.953	−0.797	−0.486	−2.546	1.209	0.868	−0.234	−0.022	0.077	7.007	1.35	127.581
12	1.974	−0.798	−0.450	−2.616	1.222	0.862	−0.238	−0.031	0.087	9.156	2.15	182.117
14	2.054	−0.855	−0.861	−2.726	1.310	1.305	−0.248	0.029	0.043	9.703	1.84	194.763

$$\log(1/IC_{50}) = +125.038 Q_{N(\alpha)} + 0.893 Q_{N(\beta)} + 96.777 P_{N–H(\alpha)}$$
$$+ 10.301 P_{N–H(\beta)} - 29.318 E_{HOMO} + 115.504 E_{LUMO}$$
$$+ 12.042\omega - 1.345\mu + 2.122 \log P - 23.942$$
$$n = 11; R^2 = 0.828; S_{reg} = 0.291;$$
$$r = 0.530; F_{statistic} = 1.203 \qquad (2)$$

where, n is the number of compounds, r is the correlation coefficient, R^2 is the determination coefficient of regression, S_{reg} is the standard deviation of regression and $F_{statistic}$ is the

Fisher's statistic [27]. The high determination coefficient ($R^2 = 0.828$) and low residuals ($S_{reg} = 11.320$) are significant. High variance inflation factor (VIF >10) (Table 6) are associated with the multicollinearity problem. Therefore, the variables with a high VIF are candidates for exclusion from the model. The improvement in Eq. (2) was carried out by omitting compound **4** as outland data from the tested compounds and replacing ω with E_{LUMO} as well as $P_{N–H(\alpha)}$ with $Q_{N(\alpha)}$. Multiple regression performed using the remaining seven parameters yielded the following model with

Table 6 VIF[a] values of theoretical QSAR equations

Independent variable	AChE		Urease	
	Equation (2)	Equation (3)	Equation (4)	Equation (5)
$Q_{N(\alpha)}$	372.737		134.265	3.438
$Q_{N(\beta)}$	1.820	1.827	1.996	1.891
$P_{N-H(\alpha)}$	318.146	2.823	269.233	
$P_{N-H(\beta)}$	67.465	4.655	71.560	4.668
E_{HOMO}	9.092	7.474	217.570	1.507
E_{LUMO}	69.705	7.836	4.045	7.370
ω	1.010		4.856	
μ	121.108	5.432	152.001	3.042
$\log P$	103.360	6.286	109.226	4.045

[a] $VIF = 1/(1 - R_i^2)$; where, R_i is the multiple correlation coefficient of the ith independent variable on all of the other independent variables

increasing of $R^2 = 0.822$ and decreasing of $S_{reg} = 0.292$ (Eq. 3).

$$\log(1/IC_{50}) = +1.002Q_{N(\beta)} + 20.819P_{N-H(\alpha)} - 1.520P_{N-H(\beta)}$$
$$+ 12.071E_{HOMO} + 47.292E_{LUMO} - 0.383\mu + 0.036\log P - 17.384$$
$$n = 10; R^2 = 0.822; S_{reg} = 0.292; r = 0.495; F_{statistic} = 1.324 \qquad (3)$$

The correlating parameters have VIF <10, thus there is no colinearity problem (Table 6). In this equation, the inhibitory potency of AChE is influenced mainly by the electronic parameters (as frontier molecular orbital energies). E_{LUMO} with the coefficient value of +47.292 has the highest contribution to $\log(1/IC_{50})$ rather than the structural parameters. The positive sings of E_{LUMO} in $\log(1/IC_{50})$ disclose that the compound with lower molecular orbital (E_{LUMO}) is indicative of higher toxicity against AChE enzyme. The correlation matrix was used to determine the interrelationship between the independent variables (Table 7). Table 7 shows that the majority of regression coefficients among; were higher than 0.70, showing that they were closely correlated. Therefore, orthogonalization of the molecular descriptors was conducted [28]. Orthogonalization of molecular descriptors is undertaken to avoid collinearity among variables and model overfitting. The high interrelationships were observed between E_{LUMO} and

E_{HOMO} ($r = +0.692$), E_{HOMO} and $P_{N-H(\alpha)}$ ($r = -0.670$), with E_{HOMO} and $\log P$ ($r = +0.627$), respectively.

The effect of hydrophobicity and polarizability in modulating inhibition activity against AChE enzyme may be due to the presence of phosphoryl ($P^{\delta+}-O^{\delta-}$), carbonyl ($C^{\delta+}-O^{\delta-}$) and amine groups ($H^{\delta+}-N^{\delta-}$); where permanent polarization was seen due to electronegativity difference between the atoms.

Urease-QSAR

Also the interaction of urease as a secondary target was investigated against the tested compounds (**1–17**) and the same procedures were carried out. The QSAR modification model based on anti-urease potency produced the following equation:

$$\log(1/IC_{50}) = +12.765Q_{N(\alpha)} + 0.678Q_{N(\beta)} + 7.064P_{N-H(\alpha)}$$
$$- 1.040P_{N-H(\beta)} - 28.525E_{HOMO} - 22.165E_{LUMO}$$
$$- 77.456\omega - 0.418\mu - 0.283\log P + 4.668$$
$$n = 12; R^2 = 0.960; S_{reg} = 0.237;$$
$$r = 0.168; F_{statistic} = 5.312 \qquad (4)$$

As a result, as shown in Table 6, the regression equation is not favorable with the VIF >10. The improvement in Eq. (4) was performed by excluding $P_{N-H(\alpha)}$ and ω. Consequently, a new multiple regression was resulted without colinearity (Eq. 5).

$$\log(1/IC_{50}) = +7.213Q_{N(\alpha)} + 0.694Q_{N(\beta)} - 2.186P_{N-H(\beta)}$$
$$- 3.165E_{HOMO} + 50.169E_{LUMO} - 0.263\mu$$
$$- 0.576\log P + 10.652$$
$$n = 12; R^2 = 0.947; S_{reg} = 0.193;$$
$$r = 0.020; F_{statistic} = 10.179 \qquad (5)$$

The model described by Eq. (5), similar to Eq. (3), depicts the share of molecular orbital energy variables in the inhibition of urease. The most effective variable in the interaction of urease and PAH derivatives was E_{LUMO} with the coefficient value of +50.169. The high interrelationship in Table 8 ($r = +0.727$) between E_{LUMO} descriptors and $P_{N-H(\beta)}$ showed that the properties of derivatives affect in the inhibition of urease. It means that polarizability and

Table 7 Correlation matrix for AChE-QSAR in Eq. (2)

Selected variables	$Q_{N(\beta)}$	$P_{N-H(\alpha)}$	$P_{N-H(\beta)}$	E_{HOMO}	E_{LUMO}	μ	$\log P$
$Q_{N(\beta)}$	1.000						
$P_{N-H(\alpha)}$	0.076	1.000					
$P_{N-H(\beta)}$	−0.300	0.192	1.000				
E_{HOMO}	−0.242	−0.670	0.107	1.000			
E_{LUMO}	−0.451	−0.472	0.325	0.692	1.000		
μ	−0.081	−0.045	0.033	0.528	0.661	1.000	
$\log P$	0.077	−0.482	−0.372	0.647	−0.670	−0.045	1.000

Table 8 Correlation matrix for urease-QSAR in Eq. (5)

Selected variables	$Q_{N(\alpha)}$	$Q_{N(\beta)}$	$P_{N-H(\beta)}$	E_{HOMO}	E_{LUMO}	μ	$\log P$
$Q_{N(\alpha)}$	1.000						
$Q_{N(\beta)}$	0.455	1.000					
$P_{N-H(\beta)}$	−0.785	−0.526	1.000				
E_{HOMO}	−0.089	−0.309	0.217	1.000			
E_{LUMO}	−0.535	−0.599	0.727	0.506	1.000		
μ	−0.157	−0.242	0.318	0.490	0.687	1.000	
$\log P$	0.352	0.046	−0.150	0.417	0.384	0.662	1.000

electrostatic interactions were formed between the N–H group were occurred with the side chain of urease enzyme.

Conclusion

New (thio)phosphorhydrazide compounds (**1**–**17**) were synthesized and characterized by spectroscopy methods. The cyclic motifs of compound **2** were further determined by X-ray crystallography. The inhibitory potencies of the selected compounds against human AChE and urease were studied. PCA–QSAR was deduced that the electronic parameters are predominated from those related to structural parameters. DFT–QSAR models for AChE ($R^2 = 0.822$ and $1.827 < VIF < 7.836$) and for urease ($R^2 = 0.947$ and $1.507 < VIF < 7.370$) models revealed that the descriptors of the E_{LUMO} parameter affect on the inhibition mechanism of enzymes. The correlation matrix of QSAR models and docking analysis confirmed that E_{LUMO} variable can control the influence of the polarizability properties of N–H functional group of PAH derivatives in the inhibition of enzymes.

References

1. A.L. Chaney, E.P. Marbach, Clin. Chem. **8**, 131 (1962)
2. R.P. Hausinger, Microbiol. Rev. **51**, 22 (1987)
3. H.L.T. Mobley, R.P. Hausinger, Microbiol. Rev. **53**, 85 (1989)
4. R.P. Hausinger, *Biochemistry of Nickel* (Plenum, New York, 1993), p. 23
5. Andrews RK, Blakeley RL, Zerner B, Lancaster JR, The Bioinorganic Chemistry of Nickel (VCH, New York) pp. 141
6. H.L.T. Mobley, M.D. Island, R.P. Hausinger, Microbiol Rev **59**, 451 (1995)
7. H. Kaltwasser, H.G. Schlegel, Anal. Biochem. **16**, 132 (1966)
8. I.J.M. Rosenstein, J.M.T. Hamilton-Miller, Crit. Rev. Microbiol. **11**, 1 (1984)
9. K.L. Sahrawat, Plant Soil **57**, 335 (1980)
10. R.L. Mulvaney, J.M. Bremner, E.A. Paul, J.N. Ladd, *Soil Biochemistry*, vol. 5 (Marcel Dekker, New York, 1981), p. 153
11. Hauck RD, Hauck RD, (Madison, WI, 1984) p. 551
12. D.A. Martens, J.M. Bremner, Soil Sci. Soc. Am. J. **48**, 302 (1984)
13. Voss RD, Hauck RD (American Society of Agronomy, Madison, 1984) p. 571
14. J.M. Bremner, M.J. Krogmeier, Proc. Natl. Acad. Sci. **85**, 4601 (1988)
15. G.W. McCarthy, J.M. Bremner, J.S. Lee, Plant Soil **127**, 269 (1990)
16. J.M. Bremner, Fert Res **42**, 321 (1995)
17. M. Pourayoubi, F. Karimi Ahmadabad, H. Eshtiagh-Hosseini, M. Kučeráková, V. Eigner, M. Dušek, Acta Cryst **C69**, 1181 (2013)
18. SPSS for Windows, Version 10.05, SPSS Inc., Bangalore, India (1999)
19. G.M. Sheldrick, Acta Cryst. A **64**, 112 (2008)
20. G.L. Ellman, K.D. Coutney, V.R. Andres, M. Featherstone, Biochem. Pharmacol. **7**, 91 (1961)
21. M.W. Weatherburn, Anal. Chem. **39**, 971 (1967)
22. K. Gholivand, A.A.E. Valmoozi, H.R. Mahzouni, S. Ghadimi, R. Rahimi, J. Agric. Food Chem. **61**, 6776 (2013)
23. S.F. Boys, F. Bernardi, Mol. Phys. **19**, 553 (1970)
24. M.J. Frisch, G.W. Trucks, H.B. Schlegel, G.E. Scuseria, M.A. Robb, J.R. Cheeseman, J.A. Montgomery, T. Vreven, K.N. Kudin, J.C. Burant, J.M. Millam, S. Iyengar, J. Tomasi, V. Barone, B. Mennucci, M. Cossi, G. Scalmani, N. Rega, G.A. Petersson, H. Nakatsuji, M. Hada, M. Ehara, K. Toyota, R. Fukuda, J. Hasegawa, M. Ishida, T. Nakajima, Y. Honda, O. Kitao, H. Nakai, M. Klene, X. Li, J.E. Knox, H.P. Hratchian, J.B. Cross, V. Bakken, C. Adamo, J. Jaramillo, R. Gomperts, R.E. Stratmann, O. Yazyev, A.J. Austin, R. Cammi, C. Pomelli, J.W. Ochterski, P.Y. Ayala, K. Morokuma, G.A. Voth, P. Salvador, J. Dannenberg, V.G. Zakrzewski, S. Dapprich, A.D. Daniels, M.C. Strain, O. Farkas, D.K. Malick, A.D. Rabuck, K. Raghavachari, J.B. Foresman, J.V. Ortiz, Q. Cui, A.G. Baboul, S. Clifford, J. Cioslowski, B. Stefanov, G. Liu, A. Liashenko, P. Piskorz, I. Komaromi, R.L. Martin, D.J. Fox, T. Keith, M.A. Al-Laham, C.Y. Peng, A. Nanayakkara, M. Challacombe, P. Gill, B. Johnson, W. Chen, M.W. Wong, C. Gonzalez, J.A. Pople, *Gaussian 03* (Gaussian Inc., Wallingford, 2005)
25. M.C. Etter, J.C. Macdonald, Acta Crystallogr. B **46**, 256 (1990)
26. S. Soltani, H. Abolhasani, A. Zarghi, A.A. Jouyban, Eur. J. Med. Chem. **45**, 2753 (2010)
27. D.R. Roy, U. Sarkar, P.K. Chattaraj, A. Mitra, J. Padmanabhan, R. Parthasarathi, V. Subramanian, S. Van Damme, P. Bultinck, Mol. Divers **10**, 119 (2006)
28. Gholivand Kh, Asadi L, Ebrahimi Valmoozi AA, Hodaii M, Sharifi M, Mazruee Kashani H, Mahzouni HR, Ghadamyari M, Kalate AA, Davari E, Salehi S, Bonsaii M RSC Adv **xx**, 1 (2016)